Environmental Science
Nano

rsc.li/es-nano

ROYAL SOCIETY
OF CHEMISTRY
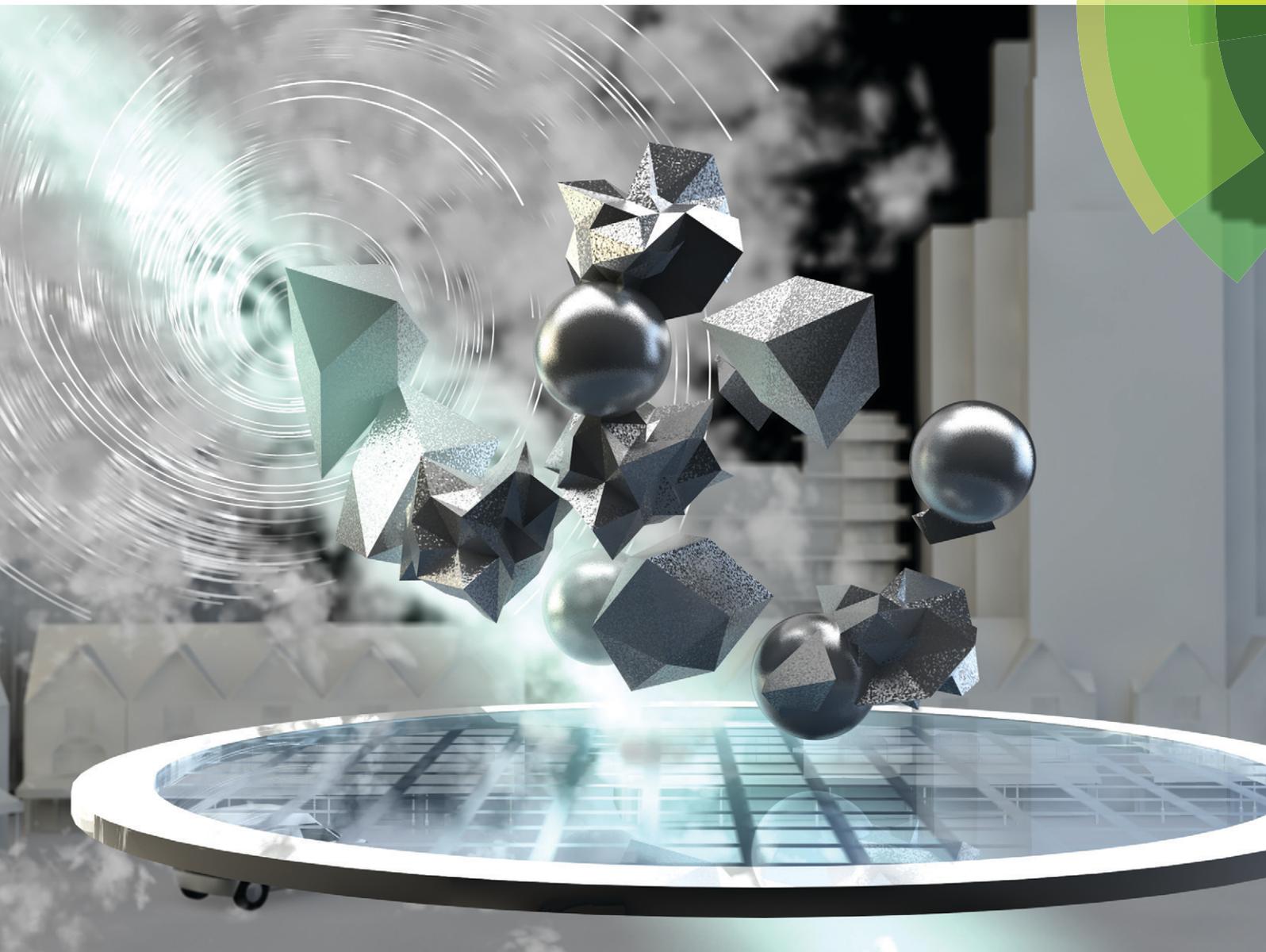
175 YEARS

PAPER
Michael F. Hochella Jr. *et al.*
Nanoparticles in road dust from impervious urban surfaces: distribution,
identification, and environmental implications

PAPER

CrossMark
click for updates

Nanoparticles in road dust from impervious urban surfaces: distribution, identification, and environmental implications†

Yi Yang,[ac] Marina Vance,[b] Feiyun Tou,[a] Andrea Tiwari,[b] Min Liu[a] and Michael F. Hochella Jr.*[cd]

Nanoparticles (NPs) resulting from urban road dust resuspension are an understudied class of pollutants in urban environments with strong potential for health hazards. The objective of this study was to investigate the heavy metal and nanoparticle content of PM2.5 generated in the laboratory using novel aerosolization of 66 road dust samples collected throughout the mega-city of Shanghai (China). The samples were characterized using an array of techniques including inductively-coupled plasma mass spectrometry, aerosol size distribution measurements, and scanning and transmission electron microscopy coupled with elemental characterization and electron diffraction. Principal metal concentrations were plotted geospatially. Results show that metals were generally enriched in aerosolized samples relative to the bulk dust. Elevated concentrations of metals were found mostly in downtown areas with intense traffic. Fe-, Pb-, Zn-, and Ba-containing NPs were identified using electron microscopy, spectroscopy, and diffraction, and we tentatively identify most of them as either engineered, incidental, or naturally occurring NPs. For example, dangerous Pb sulfide and sulfate NPs likely have an incidental origin and are also sometimes associated with Sn; we believe that these materials originated from an e-waste plant. Size distributions of most aerosolized samples presented a peak in the ultrafine range (<100 nm). We estimate that 3.2 ± 0.7 μg mg^{-1} of Shanghai road dust may become resuspended in the form of PM2.5. Aerosolization, as done in this study, seems to be a very useful approach to study NPs in dust.

Nano impact

Dust, especially road dust in urban areas, can act as a significant sink for NPs, thus posing a NP-related risk to public health. However, information of the composition, atomic structure, and characteristics of NPs in road dust is grossly lacking. Based on an array of techniques including laboratory aerosolization, size distribution measurements, ICP-MS, and SEM/TEM/EDS/SAED analyses, NPs were isolated and comprehensively characterized in street dust from Shanghai, China, presenting evidence for the concept of street dust as a sink for NPs in the urban environment and, further, as a source of atmospheric contaminants. This is the first study of its type.

Introduction

Air pollution is one of the most important global environmental issues and PM2.5, defined as particulate matter (PM)

with an aerodynamic diameter smaller than 2.5 μm, is known to cause significant damage to the environment and to human health.[1–3] Outdoor air pollution, mostly PM2.5, has been estimated to lead to 3.3 million premature deaths per year worldwide, among them 1.6 million premature deaths in China.[2,3] PM2.5 is physicochemically complex in nature, varying temporally and spatially, and is generally composed of salts, black carbon, organic matter, trace metals, biological material (*e.g.*, viruses), *etc.* In 2013, the International Agency for Research on Cancer (IARC), a specialized cancer agency of the World Health Organization (WHO), announced that PM is now considered carcinogenic to humans according to evidence of an increasing risk of lung cancer with increasing levels of exposure to PM. Compared to PM10, PM2.5 has been found more strongly related with cardiovascular and

a Key Laboratory of Geographic Information Science of the Ministry of Education, Shanghai Key lab for Urban Ecological Processes and Eco-Restoration, East China Normal University, 3663 North Zhongshan Road, Shanghai, 200062, China
b Virginia Tech Center for Sustainable Nanotechnology, Institute for Critical Technology and Applied Science, Virginia Tech, Blacksburg, VA 24061, USA
c The Center for NanoBioEarth, Department of Geosciences, Virginia Tech, Blacksburg, VA 24061, USA. E-mail: hochella@vt.edu; Fax: +1 540 231 3386; Tel: +1 540 231 6894
d Geosciences Group, Energy and Environment Directorate, Pacific Northwest National Laboratory, Richland, WA 99352, USA
† Electronic supplementary information (ESI) available. See DOI: 10.1039/c6en00056h

534 | *Environ. Sci.: Nano*, 2016, **3**, 534–544

This journal is © The Royal Society of Chemistry 2016

respiratory effects.[4] Recently more attention has been paid to ultrafine PM (<100 nm), because these nanoscale particles can penetrate through the alveolar regions of the lungs and translocate *via* blood to other organs, including the heart and brain.[5] What is most often missing from these considerations is that NPs typically show dramatically different chemical and physical properties relative to the corresponding bulk material, and insofar as is possible, this must also be considered in any studies of the impact of such particles in complex ecological environments and when taken up by organisms.[6–8]

With the rapid development of urbanization, natural surfaces (soils, rocks, vegetation, natural surface water) have dramatically shifted to impervious surfaces (buildings, roads, parking lots, sidewalks, *etc.*). In urban areas, road surfaces can accumulate particles from a wide variety of sources. Road dust is comprised of vehicle exhaust particles, de-icing salt, particles produced by other human activities in the local area, as well as biogenic and geogenic PM carried from distant to nearby locations;[9] virtually any anthropogenic and natural sources may result in the deposition of PM on roads.[10] Therefore, dust, especially road dust in urban areas, can act as a significant sink for PM2.5, including NPs.

Urban dust can be resuspended into the air, and this resuspension is suggested as a contributor of PM2.5 to other areas, along with coal combustion and motor vehicle exhausts.[11–14] Moreover, given their small size, NPs contribute little to the mass of PM in road dust, but they are significant contributors to particle number.[15] These NPs of heterogeneous physicochemical composition can be flushed by stormwater into urban sewer systems, or into streams, and thus may pose ecological risks to aquatic systems.[16–18] Until now, numerous studies have focused on the occurrence, source and risk assessment of contaminants, including PAHs, PCBs, and heavy metals[16,17] in road dust samples all over the world.

Recent research efforts have focused on road dust resuspension as one of the major sources of atmospheric particulate matter in urban environments, especially in Asia,[19–22] Europe,[23–25] and America.[26,27] The study of road dust resuspension is usually performed by sweep/vacuum collection of particles followed by sieving,[21,28] directly sampling PM on the traffic lanes,[20,23,29] or inducing resuspension in the laboratory and extracting PM through size selective inlets.[21,25,30,31] Most of the reported research has been conducted on bulk or very coarse fractions of road dust, and few studies have focused on the characterization of fine or ultrafine PM.

Shanghai is a megacity with an area of 6340 km^2 and a population of more than 24 million. With its rapid growth of population, motorization, urbanization and industrial activities, Shanghai is under serious stress from airborne contaminants, including PM2.5 and NPs. In the present study, road dust samples were collected in Shanghai from 66 well-distributed sampling sites across the city. Dust samples were then aerosolized by a novel aerosolization technique.[32] The <2.5 µm fraction of these samples was characterized using an array of techniques including ICP-MS, aerosol size distribution instrumentation, and electron microscopy techniques: scanning electron microscopy (SEM), transmission electron microscopy (TEM), scanning TEM (STEM), and selected area electron diffraction (SAED).

The objective of this work was to quantify the trace metal content and investigate the nanoparticle composition of PM2.5 generated from the resuspension of road dust collected around the city of Shanghai. Both heavy metals and nanoparticles may be indicative of existing human exposure hazards in urban environments. Specific objectives were (1) to assess geographical distribution of metal contamination in both aerosolized PM2.5 and bulk dust samples using GIS spatial analysis; (2) to investigate the size and chemical distributions of dust particles, especially in aerosolized dust samples; (3) to identify dominant NPs in aerosolized dust, and to assess whether they are engineered, incidental, or naturally occurring NPs, and (4) to estimate their environmental implications.

Materials and methods

Sample collection

Road dust samples were collected in January 2013 throughout the city of Shanghai, excluding Chongming Island (Fig. 1). Sixty-six sampling sites were selected based on their location, functional area and land use type. A detailed description of the sampling sites and their surrounding environment is presented in the Table S1† online. The Shanghai downtown district had the highest sampling density (Fig. 1 map on the right), but samples were also taken from surrounding districts (see also Table S1† online). At each sampling site, approximately 30 g of dust were dusted off the pavement along 100 m from each side of the road using a plastic brush and tray, and then mixed thoroughly to obtain a bulk sample. Samples were passed through a 0.3 mm stainless steel sieve to remove coarse particles, hair, fibers, and other large debris, and then stored in plastic bottles.

Aerosolization of dust samples

For each of 66 samples, approximately 200 mg of sieved dust sample was aerosolized in duplicate using a dry dispersion method ("disperser") based on a commercially available vacuum generator, developed by Tiwari *et al.*,[32] and operated with a 10 L min^{-1} air flow. Following aerosolization, samples were passed through a PM2.5 cyclone (URG-2000-30EN, URG Corp.) to eliminate larger particles, and the output was directed to one of three sampling trains (Fig. S1†), leading to (A) a 47 mm diameter Teflon filter with the pore size of 0.1 µm (all 66 samples), (B) a Microanalysis Particle Sampler loaded with TEM grids (nine selected samples), or (C) a 520 L chamber in which 12 selected aerosol samples were characterized using a Scanning Mobility Particle Sizer (15–650 nm size range, model 3936NL, TSI) and an Aerodynamic Particle Sizer (523 nm–20 µm size range, model 3321, TSI). Samples were selected from (B) and (C) based on their concentration
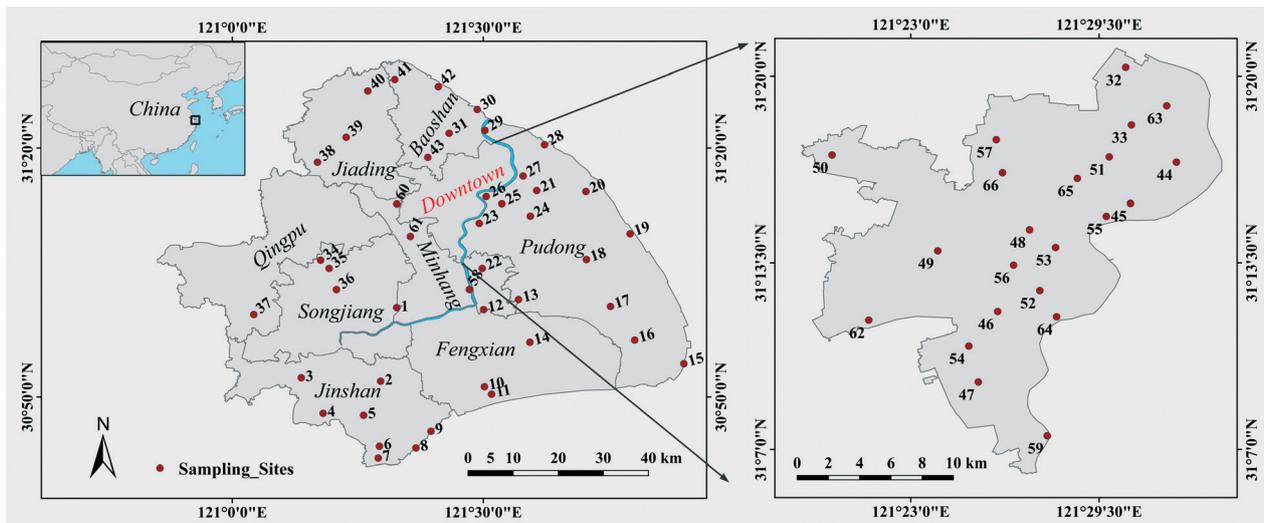
This journal is © The Royal Society of Chemistry 2016

Environ. Sci.: Nano, 2016, **3**, 534–544 | 535

Fig. 1 Sampling site distribution in Shanghai. The Shanghai downtown district had the highest sampling density (map on the right), but samples were also taken from the named districts that surround the downtown district.

of metals in the aerosolized *vs.* bulk fractions (low, medium, and high) and on whether there was sufficient sample mass for all analyses (Table S4†). A detailed description of the aerosolization methods, procedures and the QA/QC of aerosolization is presented as ESI.†

ICP-MS analysis

Bulk and aerosolized dust samples were predigested using HNO_3 and H_2O_2, and further microwave digested according to EPA Method 3050B.[33] This method is considered satisfactory for most metals but is inefficient for titanium oxides, which are insoluble even under strong acidic conditions. Trace element concentrations including Ti, V, Cr, Fe, Mn, Co, Ni, Cu, Zn, As, Sr, Mo, Ag, Cd, Sn, Ba and Pb were analyzed using an Thermo Electron X-Series inductively coupled plasma mass spectrometer (ICP-MS) per standard method 3125-B.[33] Calibration standards (high-purity standards) were prepared in a matrix of 2% nitric acid by volume in duplicate. The detection limit for each element is listed in Table S2 in the ESI.†

Electron microscopy analysis

Bulk dust samples were investigated using an environmental scanning electron microscope (ESEM, FEI Quanta 600 FEG) equipped with an energy-dispersive X-ray spectrometer (EDS, QUANTAX 400, Bruker). The backscattered electron (BSE) mode was used to provide visual information based on the contrast between phases of different atomic numbers (Z). For example, a particle containing lead (atomic number 82, atomic mass 207) is significantly brighter than one of carbon (atomic number 6, atomic mass 12). Selected aerosolized samples were further investigated using a scanning transmission electron microscope operating at 200 kV and equipped with a silicon drift detector-based EDS system (JEM 2100 TEM/Scanning-TEM, JEOL Corporation). Electron diffraction

patterns of the crystalline and semi-crystalline phases were recorded in selected area electron diffraction (SAED) mode.

GIS methods

To obtain the spatial distribution maps of the heavy metals in urban dust, which indicate the spatial variability and potential hot spots, IDW (Inverse Distance Weighted) software was applied to interpolate the heavy metal concentrations from sampling sites to area maps. ArcMap 10.1 software was used for the mapping and spatial analysis.

Results and discussion

Metal concentrations in aerosolized and bulk dust

During the aerosolization of dust samples, we essentially removed particles larger than 2.5 μm and recovered only the fraction that can be resuspended relatively easily during everyday urban activities. Metal concentrations (Fig. S2†) and GIS distributions (Fig. S3†) of metals, as well as the grain size distribution (Fig. S4†) in bulk samples, are discussed in the ESI.† Compared to bulk samples, aerosolized dust shows a generally similar pattern of metal concentrations (Fig. S5†). Iron is the metal present in highest concentration, ranging from approximately 11 000 to 94 000 mg kg^{-1} with an average of 45 968 mg kg^{-1}. Zn, Mn, Cu and Ba follow with average concentrations of 1836 mg kg^{-1}, 1160 mg kg^{-1}, 1138 mg kg^{-1} and 833 mg kg^{-1}, respectively. Lead has concentrations in the range of 42–9626 mg kg^{-1} with an average of 566 mg kg^{-1}.

The spatial distribution of each metal is shown on the GIS maps in Fig. 2. Cr, Fe, Mn, Co and Ni all present a similar distribution pattern with hot spots in western Shanghai, namely in the Baoshan, Minhang, Songjiang, and Jinshan districts and downtown. V presents a similar GIS distribution pattern with As, with hotspots in the Pudong, Fengxian, and Jinshan districts and downtown. Zn and Ba present similar patterns with hotspots mostly in the downtown area. The
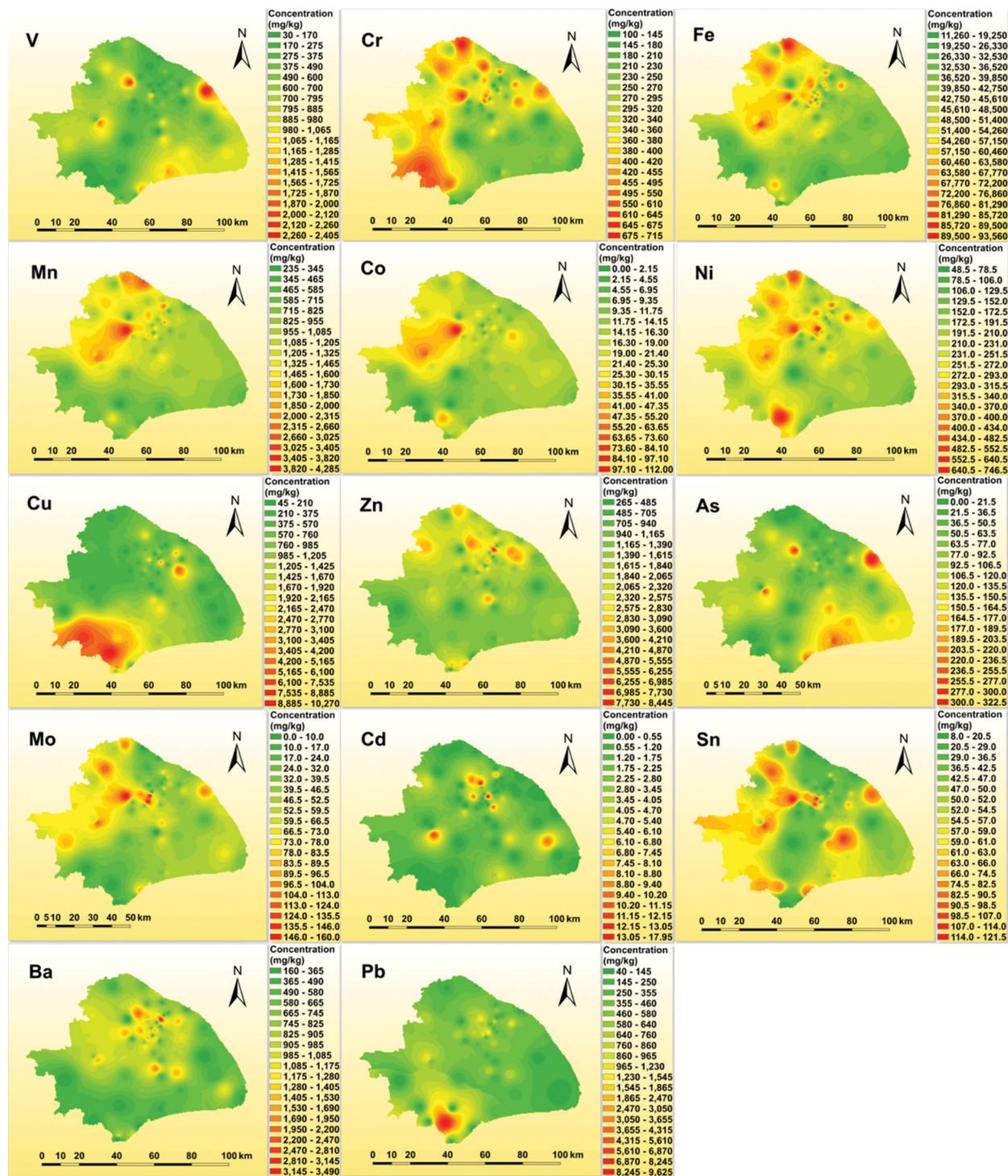
Fig. 2 GIS maps of metals in the aerosolized dust samples in Shanghai.

occurrence of elevated concentrations of these metals in the downtown area can be attributed to PM2.5 release from slow-moving vehicles, as vehicle emissions are typically characterized by trace metals such as Cr, Fe, Cu, Ba (brake source), and Zn (tire wear).[26,34–36] This is in agreement with the traffic volume distribution pattern according to the data from Shanghai Road Administration Bureau that the downtown

area has the highest traffic volume (Fig. S6† online). The GIS maps for Sn and Mo show elevated concentrations through-out the western part of Shanghai. Cu presents a similar distri-bution pattern to Pb, with sharply elevated levels in the Jinshan district and downtown. Additionally, Cd also pre-sents a similar spatial distribution pattern to Pb in the down-town area. However, Pb has an extremely high concentration

This journal is © The Royal Society of Chemistry 2016

Environ. Sci.: Nano, 2016, 3, 534–544 | 537

in sample 5 collected near an e-waste plant in the Jinshan district; this high concentration is also observed in bulk dust samples. The highest Pb concentration goes up to 3192 mg kg^{-1} in bulk dust sample 5, and this concentration is close to the highest concentration reported in Xi'an city in China,[37] and higher than those reported in other cities worldwide.[38]

Furthermore, a principal component analysis (PCA) following a varimax rotation method was applied for the source apportionment of metals in the aerosolized dust samples (Table S3† online).[39,40] Four PCs were identified, indicating the local industry and vehicle emissions as the dominant sources for the aerosolized dust in Shanghai (see the detailed description in the ESI† online).

Concentrations of certain metals—Mn, Fe, Zn, Ba and Pb—in aerosolized dust samples have strong positive correlations ($p < 0.05$) to their corresponding concentrations in bulk samples as shown in Fig. S7;† i.e., the higher concentrations of these metals in bulk samples, the higher their concentrations are in aerosolized samples. Furthermore, all metals analyzed are, in general, enriched during aerosolization, i.e., they are present in higher concentrations in aerosolized than bulk dust samples (Fig. 3). To further elucidate the enrichment of metals in fine particles, the aerosol enrichment factor was introduced; this is a ratio of metal concentrations in aerosol over bulk dust samples, represented by

$$ef = \frac{C_{aerosol}}{C_{bulk}}$$

($C_{aerosol}$ and C_{bulk} represent the concentration of each element in aerosolized and bulk dust samples, respectively). V, Cr, Ni, Cu, As, Mo, Ag, and Sn show high enrichment factors with average ef > 5. The high ef values indicate that those metals are more likely to be present in the fraction of dust samples that can be easily aerosolized (Dp < 2.5 μm). It is also noticeable that for these metals with high ef values, there are no significant correlations between their concentrations in aerosolized and bulk dust samples, indicating that

these may originate from distinct sources. Average ef values per sampling site are presented in Table S5† online.

Size distribution of the aerosolized dust samples

The aerosolization of the street dust in the laboratory resulted in aerosol emission factors ranging from 3.3×10^6 to 4.7×10^7 particles per mg of dust, with an average of $(1.9 \pm 0.4) \times 10^7$ PM2.5 particles per mg of dust. By assuming spherical shape and unit aerosol density, we estimate an average mass emission factor of 3.2 ± 0.7 μg PM2.5 particles per mg of dust. We observed two main size distribution patterns (Fig. 4).

The majority of analyzed samples (9 out of 12) presented a major peak in the ultrafine (<100 nm) range at 34 ± 1 nm, and a secondary peak at 914 ± 46 nm (Fig. 4a). Three samples presented overlapping peaks in the 200–400 nm range and in the 1000 nm range (main peak at 350 ± 53 nm), but no peaks in the ultrafine range (Fig. 4b). Aerosol medians, modes, and emission factors for each sampling site are presented in Table S4† online.

The dispersion technique used in this work has previously been used by us to aerosolize bovine serum albumin (BSA) and mannitol,[41] as well as TiO$_2$, CeO$_2$,[32] and C$_{60}$ (ref. 32 and 42) nanoparticle powders. Size distributions in Fig. 4 do not resemble those reported in these studies, which reported unimodal size distributions (except for TiO$_2$). The minimum particle size for the aerosolized materials in these previous studies correlates with the primary particle size (several microns for BSA and mannitol, 30 nm for TiO$_2$, 15 nm for CeO$_2$), except for C$_{60}$, which is molecular in nature. This suggests that the disperser partially deagglomerated these materials, but did not fracture primary particles.

This dispersion method deagglomerates incoming particles via collision with each other and with the interior walls of the disperser. Most of these collisions happen at particle
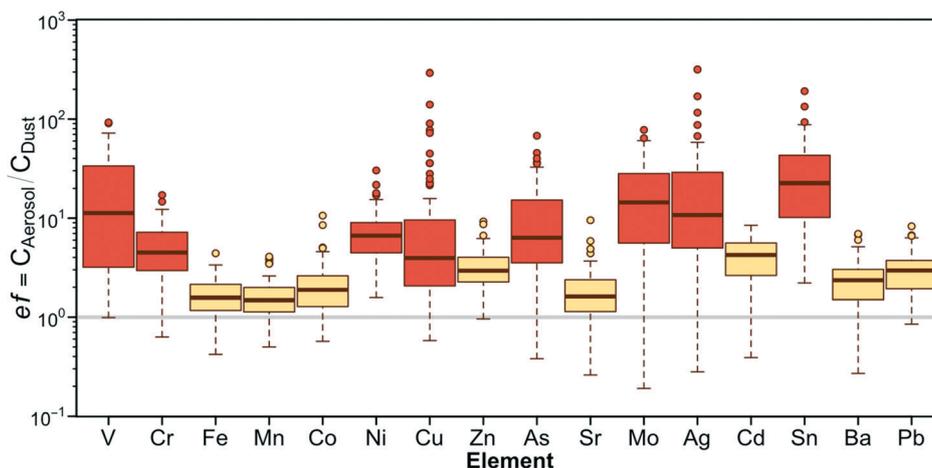

Fig. 3 Ratios of the concentration of metals in aerosolized samples over bulk dust, representing the overall enrichment of metals in aerosolized samples (or "aerosol enrichment factor", ef). A horizontal line was added to the ratio of 1 to represent the hypothetical point in which there would be no significant difference between bulk and aerosolized samples. An ef greater than one signifies that aerosolized samples contain a relatively higher concentration of said metal than bulk dust samples, which may indicate that said metal is more likely to be present in particles smaller than 2.5 μm. Groups with average ef > 5 are highlighted in red (darker shade).

538 | Environ. Sci.: Nano, 2016, 3, 534–544

This journal is © The Royal Society of Chemistry 2016
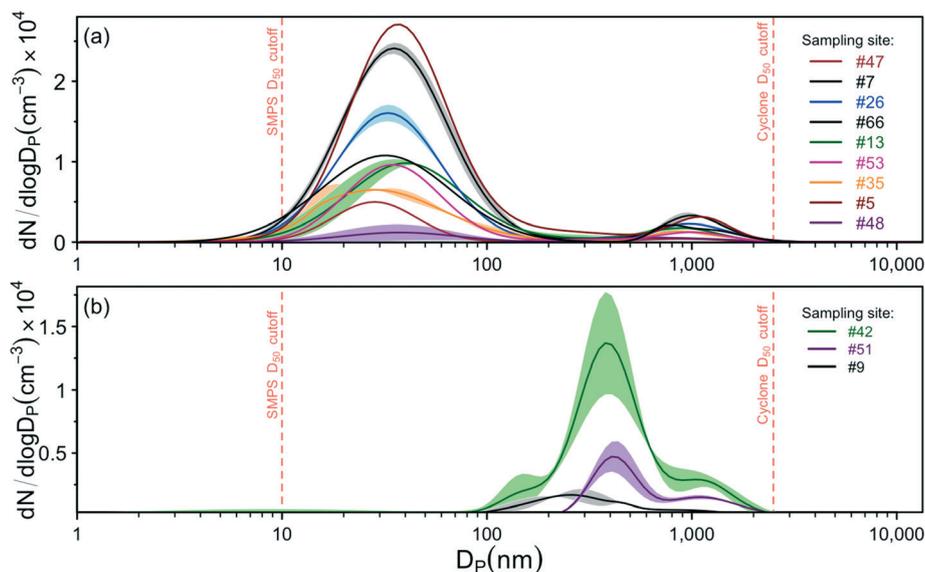
Fig. 4 Aerosol size distributions of aerosolized samples presenting a primary peak <100 nm (a) and those with a primary peak >100 nm (b). Shaded areas represent standard errors to the mean values. Curves with no shaded regions represent situations in which only one sample was aerosolized due to insufficient sample mass for replicates. The residual standard deviation (RSD) at the peak measurement in site #42 (the broadest distribution) is 30%.

speeds below 10 m s^{-1},[41] which is a realistic air speed within an urban area.[43] We conclude that the dispersion acted to deagglomerate the dust in this study but is not likely to have fractured constituent particles.

Dominant nanoparticles observed in aerosolized dust samples

Based on their metal concentrations, samples 5, 7, 26, 42, 47, 48, 51, 53 and 66 were further investigated using SEM and TEM. In addition to soot and amorphous silica particles, Fe-, Pb-, Ba-containing NPs and other metal oxide NPs were found to be dominant NPs in aerosolized dust samples.

Iron oxides

We found the iron oxides magnetite (Fe_3O_4), hematite (Fe_2O_3), goethite ($FeO(OH)$), and ferrihydrite (a poorly crystalline ferric oxyhydroxide) in aerosolized dust samples with many grains ranging down in size to a few tens of nanometers or less. As shown in Fig. S8,† magnetite aggregates with different morphologies and primary sizes were identified with d-spacings of 4.8 Å and 2.96 Å, which match the (111) and (220) lattice planes of magnetite. These particles (Fig. S8B†) show clearly an octahedral or cubic shape, with growth surfaces terminating on serrated (111) faces (Fig. S8B2†). Scanning TEM revealed these magnetite particles to be coated with a carbon-rich film, and show strong association with minor amounts of other metals, such as Cr, Ni, Cu and Zn. In contrast, as shown in Fig. S8C,† magnetite aggregates were observed with primary spherical particles in the size of 50–600 nm. The largest particles are surrounded by small spherules (50–200 nm), and STEM/EDS analysis shows that these are associated with minor amounts of Mn, Cu, Zn, and

trace amounts of Ni and Pb. Additionally, hematite aggregates were found to be composed of very small primary particles, ranging from a few nm to 20 nm, with d-spacings of 3.70, 2.71, 2.52, 2.28, 2.21 Å, which match d-spacings of the (012), (104), (110), (006) and (113) hematite planes, respectively (Fig. S9A†).

Magnetic particles are often found in coal fly ash[44] and diesel exhaust.[45] These combustion related magnetite particles are usually spherical and their sizes vary depending on the combustion temperature and fuel type.[44,46,47] The occurrence of magnetite and hematite in coal fly ash may be due to the transformation of pyrite (FeS_2) and szomolnokite ($FeSO_4 \cdot H_2O$) during coal combustion.[44] A recent study on magnetic PM shows that the grain size of the emitted particles deceases from steel works, to coal combustion, to vehicle exhaust, and that magnetite is the dominant inorganic PM in these occurrences.[48] In addition to combustion related particles, most magnetic particles derive from vehicle emissions via abrasion/corrosion of engine or vehicle body material. They are typically in the form of non-spherical aggregates.[49,50] We found abundant spherical magnetic NPs which are probably derived from fuel combustion processes. The non-spherical magnetite nanoparticles (Fig. S8A and B†) could also be related to vehicle emission,[46,47] but biogenic magnetite cannot be excluded, especially for the case in Fig. S8A,† as biogenic magnetite is usually in the nano-scale with high crystallinity.[51] Naturally occurring hematite also cannot be ruled out, as it is exceptionally common in soils around the world.[8,52]

Other nano-iron oxides, such as ferrihydrite particles (most likely naturally occurring due to its ubiquity in soils and surface waters, although incidental origins cannot be ruled out), were also identified by the d-spacing of 2.5 and

This journal is © The Royal Society of Chemistry 2016

Environ. Sci.: Nano, 2016, **3**, 534–544 | 539

1.5 Å according to the SAED pattern (Fig. S9B2†). Iron-rich incidental fly ash particles are spherical (Fig. S9C†) and ubiquitous in all the aerosolized samples investigated. Geothite aggregates with a schwertmannite-like "hedge-hog" morphology[8,52,62] were also found in dust samples (Fig. S9D†). These iron rich particles show a sharp electron diffraction pattern with *d*-spacings of 4.98, 2.70 and 2.58 Å matching geothite (Fig. S9D2†). As shown in Fig. S9D3,† the goethite needles are formed by nanorods from a few nanometers to 20 nm or so in length, and EDS analyses also show that Mn, Ni and Zn are also associated with these needles. Such goethite morphologies are very common in soils and many other geologic environments.[8,62]

Lead nanoparticles

Lead was found in elevated concentrations in many samples; its maximum concentration in both aerosolized and bulk dust occurred at site 5. Many types of Pb-containing phases, not surprisingly sulfides and sulfates due to the tremendous chemical affinity between lead and sulfur, are likely all incidental particles as described below. Details were revealed by SEM and TEM investigation. Because the contrast observed in SEM-based BSE images is the result of differences in Z, particles containing Pb (very high Z) appear much brighter. Pb-rich particles in different sizes were ubiquitous in dust samples from site 5 as shown in Fig. 5. Using EDS, Pb and S
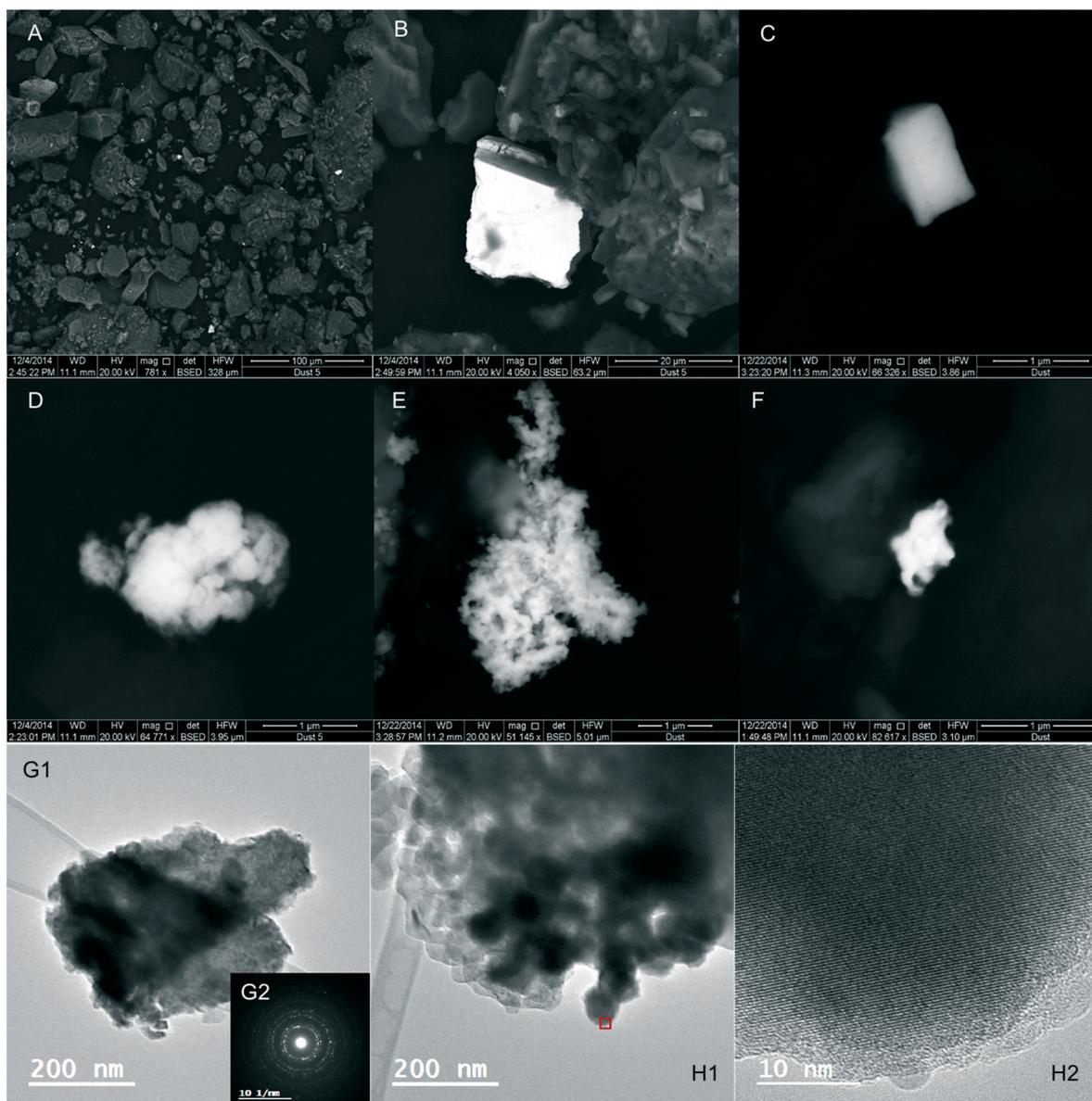

Fig. 5 Various lead-containing particles in bulk dust and aerosolized dust samples from site 5. A: BS SEM image shows the distribution of lead-rich particles; B–C: BS SEM images show typical PbS particles both in the bulk dust and aerosolized samples; D–F: BS SEM images, showing Pb-rich particles associated with Sn; G1–2: TEM and SAED images show $PbSO_4$ associated with $SnSO_4$; H1–2: TEM images show $PbSO_4$ aggregates with primary size <50 nm and H2 is the magnification of the selected area in H1.

540 | *Environ. Sci.: Nano*, 2016, **3**, 534–544

This journal is © The Royal Society of Chemistry 2016

were found to be dominant elements, which suggests the existence of PbS in the dust from site 5 (Fig. 5B). Sn was also found in those Pb-rich particles as well as in other samples (Fig. 5D–F). Using TEM coupled with EDS and SAED, we show that the co-existence of Pb and Sn is attributed to the occurrence of $PbSO_4$ and $SnO_2/SnSO_4$ (Fig. 5G), and Pb adsorbed onto $SnSO_4$.

It is important to note that site 5 is located near an e-waste recycling plant. E-waste is hazardous and contains many toxic components, including lead. Lead is predominantly found in the glass of cathode ray tubes (CRTs), solders, and in mobile phones. For example, a large CRT can contain up to 3 kg of lead.[53] Lead sulfate has been one of the most effective and commonly used stabilizers in PVC sheathing for cables and wires. Lead and tin solders have been widely used in electronics.[54] In a recent study, Julander et al.[55] reported a linear correlation between lead concentrations in the inhalable aerosol fraction and in blood, plasma, or urine in workers at e-waste recycling plants. In the present study, the concentration of lead was 3.1 ± 0.2 times higher in aerosolized PM2.5 than in bulk street dust and the concentration of lead in the PM 2.5 of site 5 was found to be more than 9000 $\mu g\ g^{-1}$, thus posing the potential for extremely high risk to the local population.

In addition to PbS and Pb–Sn rich NPs, $PbSO_4$ and $PbSO_4$ associated with Sb were also investigated in dust samples. Sb has been mainly used in alloys for batteries, plain bearings and solders, and it has been suggested as a tracer for brake wear.[26] For example, Fig. 5H shows a $PbSO_4$ aggregate with primary particles in the size of 40–80 nm found in dust taken from a university campus (site 51), which is likely attributed to atmospheric deposition. In a study applying X-ray absorption fine structure (XAFS), $PbSO_4$ was found as a major chemical phase of lead in PM10 samples in Shanghai and major sources of lead were attributed to coal combustion, metallurgic dusts and automobile exhaust.[56]

Other dominant nanoparticles

Barite ($BaSO_4$) nanoparticles (Fig. S10A;† could be mined minerals or synthetic materials) were ubiquitous in dust samples, which was confirmed by EDS detection and d-spacing values of 4.34, 3.89, 3.30, and 3.11 Å, identified by SAED (Fig. S10A3†). They are typically in a size range of 10 nm up to a few microns as shown in Fig. S10(A1 and A2).† Barite is commonly used as a weighting agent for drilling fluids in oil and gas exploration, and it can also be used in paints and plastics, soundproofing in engine compartments, automobile coatings, friction products for automobiles and trucks, etc. Fig. S9A2† shows barite particles ranging from 200 to 300 nm that are associated with Fe, Co, Cu and Sr.

TiO_2 and ZnO nanoparticles, which are common among engineered NPs, were also commonly found in Shanghai dust samples. The ZnO could be originating from vehicle emissions, because engineered ZnO nanoparticles are commonly added to tires as an activator of the vulcanization process.

TiO_2, identified as rutile aggregates, were also discovered in dust samples. Additionally, zinc and iron sulfide NPs were also found.

Calcium-containing particles, such as $CaCO_3$, $CaSO_4$ and CaO, as naturally occurring and/or incidental particles, were ubiquitous in dust samples. Moreover, calcium phosphate in the form of hydroxyapatite, $Ca_5(PO_4)_3(OH)$, was identified in aerosolized dust samples (Fig. S10B†). Hydroxyapatite is the main inorganic constituent of bone and teeth. The cytotoxicity of hydroxyapatite is size and shape-dependent;[57] hydroxyapatite NPs can induce cell death and, when inhaled, they can cause adverse biophysical effects on pulmonary surfactants.[58] As shown in Fig. S10B1,† hydroxyapatite NPs were present in sizes of 30–90 nm in rod and spherical shapes and were associated with trace amounts of iron, cobalt and zinc.

Incidental soot and soot-like aggregates were also ubiquitous in all samples investigated, with primary particle sizes ranging from 40 to 120 nm (Fig. S10C†). A typical onion-like structure of graphitic layers with an amorphous structure was observed (Fig. S10C2†). Other ubiquitous soot-like materials in smaller particle sizes (ranging from a few nm to 60 nm) were found to be aggregates of amorphous silica (Fig. S10D†), using EDS and SAED. Amorphous silica is used in a variety of products, such as in tire compounds, as fillers in the rubber industry, as free-flow and anti-caking agents in powder materials, and they are also widely used in toothpaste additives, paints, silicon rubber, insulation material, liquid systems in coatings, adhesives, printing inks, plastisol car undercoats, and cosmetics.[59] The ubiquity of amorphous silica in road dust samples suggests that it is likely to have originated from the abrasion of vehicle tires. Crystalline silica has been classified as a known hazardous and carcinogenic air pollutant and amorphous silica is known to be less toxic. Nevertheless, severe lung inflammation[60] and cardiovascular toxicity[61] have been reportedly induced by ultrafine amorphous silica particles. Ultrafine silica is naturally occurring, and is common in soils and sediments,[63] but it is synthesized for industrial uses.

Conclusions and environmental implications

In this work, based on an array of techniques including laboratory aerosolization, size distribution measurements, ICP-MS, and SEM/TEM/EDS/SAED analyses, we demonstrate the wealth of information that can be obtained from collecting and analyzing street dust and nanoparticles contained therein. This information is used to understand not only atmospheric resuspension processes, but also to assess the importance of the nanoparticles as urban environmental pollutants consisting of a mixture of engineered, incidental, and naturally-occurring nanoparticles. Further, street dust may become a valuable resource with respect to epidemiological studies of urban public health: it is simple to collect (compared to PM2.5 atmospheric sampling), it may be collected from a large number of sites nearly simultaneously (unlike

This journal is © The Royal Society of Chemistry 2016

Environ. Sci.: Nano, 2016, 3, 534–544 | 541

all but the largest air-sampling campaigns), it is reflective of surrounding environmental hazards, it is time-integrated (representing the local environment in the past few days to weeks, depending on the meteorological conditions), and it is reflective of potential local public exposures. Dust content is also clearly influenced by atmospheric deposition, and may thus reflect public health hazards of local, regional, and even global scales.

Dust aerosolization, as done in this study, may be a useful way to examine the composition and characteristics of nanoparticles contained in the dust, further providing information on potentially resuspended NPs. Street dust aerosolization brings two important advantages over bulk street dust analysis: (1) from an exposure science standpoint, this technique makes it possible to probe into the dust fraction that can be resuspended and inhaled; and (2) from an environmental nanoscience standpoint, it enables electron microscopy analyses of the nanoscale components of dust, which, without the aerosolization step, may be completely obscured by large particles in bulk samples. The volume distribution of bulk dust shown in Fig. S4† demonstrates this point: particles too large to be suitable for analysis by electron microscopy make up a significant portion of the total sample volume. Lacking aerosolization to separate the bulk dust into its constituents, nanoscale particles would not be observable *via* microscopy. This technique may be especially informative for samples collected in complex and large urban areas, such as Shanghai, which are likely to contain a higher diversity of nanoparticles, including those that have not been included in the present study, such as NPs that have organic components, as well as Pt-group elements which would be expected from catalytic converters.

Clearly, as dust is re-suspended by anthropogenic activity and/or natural phenomena (windy conditions), its nano-constituents pose a public health hazard *via* inhalation due to the NPs' deep penetration into the alveolar regions of the lung.[5] As discussed above, certain metals were enriched in the aerosolized dust relative to the bulk dust. Elements with ef values higher than 1 indicate that inhalation exposures to that particular metal may be significantly higher than the mass ratio of that element in bulk dust would suggest. Various NPs were identified in the aerosolized dust samples, including Fe-, Pb-, Ba-, and Zn-containing particles, and other nano-sized particles. These NPs were found mostly as aggregates in a wide size range from nanometers up to microns. Larger aggregates could be broken down into smaller NPs under different meteorological conditions and traffic activities, thus posing a potentially higher environmental risk. Furthermore, the size distribution of aerosolized samples showed that the majority of samples presented a major peak in the ultrafine (<100 nm) range, indicating definite inhalation health risks. In addition, we estimate an average of 3.2 ± 0.7 μg mg^{-1} of dust to become resuspended in the form of PM2.5 in the city of Shanghai. This information can be used to inform air quality models and policy makers interested in the contribution of road dust to environmental pollution in large cities.

Acknowledgements

References

1 R. Beelen, O. Raaschou-Nielsen and M. Stafoggia, *et al.* Effects of long-term exposure to air pollution onnatural-cause mortality: an analysis of 22 European cohorts within the multicentre ESCAPE project, *Lancet*, 2014, **383**, 785–795.

2 J. Lelieveld, J. S. Evans, M. Fnails, D. Giannadaki and A. Pozzer, The contribution of outdoor air pollution sources to premature mortality on a global scale, *Nature*, 2015, **525**(7569), 367–371.

3 R. A. Rohde and R. A. Muller, Air Pollution in China: Mapping of Concentrations and Sources, *PLoS One*, 2015, **10**(8), e0135749.

4 M. L. Bell, Assessment of the health impacts of particulate matter characteristics, *Res. Rep. - Health Eff. Inst.*, 2012, **161**, 5–38.

5 M. Geiser and W. G. Kreyling, Deposition and biokinetics of inhaled nanoparticles, *Part. Fibre Toxicol.*, 2010, 7, 1–17.

6 M. R. Wiesner, G. V. Lowry, K. L. Jones, M. F. Hochella, R. T. Di Giulio, E. Casman and E. S. Bernhardt, Decreasing uncertainties in assessing environmental exposure, risk and ecological implications of nanomaterials, *Environ. Sci. Technol.*, 2009, **43**, 6458–6462.

7 M. R. Wiesner, G. V. Lowry, E. Casman, P. Bertsch, C. Matson, R. T. Di Giulio, J. Liu and M. F. Hochella, Meditations on the ubiquity and mutability of nano-sized materials in the environment, *ACS Nano*, 2011, 5, 8466–8470.

8 M. F. Hochella, D. Aruguete, B. Kim and A. S. Madden, Naturally Occurring Inorganic Nanoparticles: General Assessment and a Global Budget for One of Earth's Last Unexplored Geochemical Components, in: *Nature's Nanostructures*, ed. A. S. Barnard and H. Guo, Pan Stanford Publishing, Singapore, 2012, pp. 1–42.

9 A. Thorpe and R. M. Harrison, Sources and properties of non-exhaust particulate matter from road traffic: a review, *Sci. Total Environ.*, 2008, **400**(1–3), 270–282.

10 Fine particulate matter (PM2.5) in the United Kingdom; Air Quality Expert Group: Landon, 2012, www.gov.uk/

542 | *Environ. Sci.: Nano*, 2016, **3**, 534–544

This journal is © The Royal Society of Chemistry 2016

government/uploads/system/uploads/attachment_data/file/69635/pb13837-aqeg-fine-particle-matter-20121220.pdf.

11 P. S. Zhao, Y. C. Feng, T. Zhu and J. H. Wu, Characterizations of resuspended dust in six cities of North China, *Atmos. Environ.*, 2006, **40**(30), 5807–5814.

12 F. Amato, X. Querol, C. Johansson, C. Nagl and A. Alastuey, A review on the effectiveness of street sweeping, washing and dust suppressants as urban PM control methods, *Sci. Total Environ.*, 2010, **408**(16), 3070–3084.

13 J. Gu, Z. Bai, W. Li, L. Wu, A. Liu, H. Dong and Y. Xie, Chemical composition of PM2.5 during winter in Tianjin, China, *Particuology*, 2011, **9**(3), 215–221.

14 F. Wang, T. Lin, Y. Li, T. Ji, C. Ma and Z. Guo, Sources of polycyclic aromatic hydrocarbons in PM2.5 over the East China Sea, a downwind domain of East Asian continental outflow, *Atmos. Environ.*, 2014, **92**, 484–492.

15 *Understanding the Health Effects of Ambient Ultrafine Particles*, Health Effects Institute, Boston MA, 2013, http://pubs.healtheffects.org/getfile.php?u=893.

16 B. G. Wei and L. S. Yang, A review of heavy metal contaminations in urban soils, urban road dusts and agricultural soils from China, *Microchem. J.*, 2010, **94**(2), 99–107.

17 T. Yang, Q. Liu, H. Li, Q. Zeng and L. Chan, Anthropogenic magnetic particles and heavy metals in the road dust: Magnetic identification and its implications, *Atmos. Environ.*, 2010, **44**(9), 1175–1185.

18 A. Liu, L. Liu, D. Li and Y. Guan, Characterizing heavy metal build-up on urban road surfaces: Implication for stormwater reuse, *Sci. Total Environ.*, 2015, **515**, 20–29.

19 P. Pant and R. M. Harrison, Estimation of the contribution of road traffic emissions to particulate matter concentrations from field measurements: A review, *Atmos. Environ.*, 2013, 77, 78–97.

20 P. Pant, S. J. Baker, A. Shukla, C. Maikawa, K. J. Godri Pollitt and R. Harrison, The PM10 fraction of road dust in the UK and India: Characterization, source profiles and oxidative potential, *Sci. Total Environ.*, 2015, **530-531**, 445–452.

21 J. Chen, W. Wang, H. Liu and L. Ren, Determination of road dust loadings and chemical characteristics using resuspension, *Environ. Monit. Assess.*, 2012, **184**, 1693–1709.

22 T. T. Duong and B. K. Lee, Determining contamination level of heavy metals in road dust from busy traffic areas with different characteristics, *J. Environ. Manage.*, 2011, **92**(3), 554–562.

23 F. Amato, M. Pandolfi, T. Moreno, M. Furger, J. Pey, A. Alastuey, N. Bukowiecki, A. S. H. Prevot, U. Baltensperger and X. Querol, Sources and variability of inhalable road dust particles in three European cities, *Atmos. Environ.*, 2011, **45**, 6777–6787.

24 N. Bukowiecki, P. Lienemann, M. Hill, M. Furger, A. Richard, F. Amato, A. S. H. Prevot, U. Baltensperger, B. Buchmann and R. Gehrig, PM10 emission factors for non-exhaust particles generated by road traffic in an urban street canyon and along a freeway in Switzerland, *Atmos. Environ.*, 2010, **44**, 2330–2340.

25 D. Martuzevicius, L. Kliucininkas, T. Prasauskas, E. Krugly, V. Kauneliene and B. Strandberg, Resuspension of particulate matter and PAHs from street dust, *Atmos. Environ.*, 2011, **45**, 310–317.

26 J. J. Schauer, G. C. Lough, M. M. Shafer, W. C. Christensen, M. F. Arndt, J. T. DeMinter and J. S. Park, Characterization of Emissions of Metals Emitted from Motor Vehicles, *HEI Research Report*, Health Effects Institute, Boston, MA, 2006, p. 133.

27 M. D. Hays, S. H. Cho, R. Baldauf, J. J. Schauer and M. Shafer, Particle size distributions of metal and non-metal elements in an urban near-highway environment, *Atmos. Environ.*, 2011, **45**, 925–934.

28 W. Birmili, A. G. Allen, F. Bary and R. M. Harrison, Trace Metal Concentrations and Water Solubility in Size-Fractionated Atmospheric Particles and Influence of Road Traffic, *Environ. Sci. Technol.*, 2006, **40**, 1144–1153.

29 F. Amato, M. Pandolfi, M. Viana, X. Querol, A. Alastuey and T. Moreno, Spatial and chemical patterns of PM10 in road dust deposited in urban environment, *Atmos. Environ.*, 2009, **465**(43), 1650–1659.

30 J. C. Chow, J. G. Watson, H. Kuhns, V. Etyemezian, D. H. Lowenthal, D. Crow, S. D. Kohl, J. P. Engelbrecht and M. C. Green, Source profiles for industrial, mobile, and area sources in the Big Bend Regional Aerosol Visibility and Observational study, *Chemosphere*, 2004, **54**, 185–208.

31 P. Zhao, Y. Feng, T. Zhu and J. Wu, Characterizations of resuspended dust in six cities of North China, *Atmos. Environ.*, 2006, **40**, 5807–5814.

32 A. J. Tiwari, C. G. Fields and L. C. Marr, A cost-effective method of aerosolizing dry powdered nanoparticles, *Aerosol Sci. Technol.*, 2013, **47**(11), 1267–1275.

33 L. S. Clesceri, A. E. Greenberg and A. D. Eaton, *Standard Methods for the Examination of Water and Wastewater*, 20th edn, American Public Health Association, Washington DC, 1999.

34 P. Wahlin, R. Berkowicz and F. Palmgren, Characterisation of traffic-generated particulate matter in Copenhagen, *Atmos. Environ.*, 2006, **40**, 2151–2159.

35 J. K. Gietl, R. Lawrence, A. J. Thorpe and R. M. Harrison, Identification of brake wear particles and derivation of a quantitative tracer for brake dust at a major road, *Atmos. Environ.*, 2010, **44**, 141–146.

36 J. H. J. Hulskotte, G. D. Roskam and H. A. C. Denier Van Der Gon, Elemental composition of current automotive braking materials and derived air emission factors, *Atmos. Environ.*, 2014, **99**, 436–445.

37 Y. Han, P. Du, J. Cao and E. S. Posmentier, Multivariate analysis of heavy metal contamination in urban dusts of Xi'an, *Sci. Total Environ.*, 2006, **355**, 176–186.

38 I. Nwabueze, J. Entwistle and J. R. Dean, Human health risk from Pb in urban street dust in northern UK cities, *Environ. Chem. Lett.*, 2014, **12**(1), 209–218.

39 A. K. Pathak, S. Yadav, P. Kumar and R. Kumar, Source apportionment and spatial–temporal variations in the metal content of surface dust collected from an industrial area adjoining Delhi, *Sci. Total Environ.*, 2013, **443**, 662–672.

This journal is © The Royal Society of Chemistry 2016

Environ. Sci.: Nano, 2016, **3**, 534–544 | 543

40 Y. Song, J. Ji, Z. Yang, X. Yuan, C. Mao, R. L. Frost and G. A. Ayoko, Geochemical behavior assessment and apportionment of heavy metal contaminants in the bottom sediments of lower reach of Changjiang River, *Catena*, 2011, **85**, 73–81.

41 P. Tang, D. F. Fletcher, H. K. Chan and J. A. Raper, Simple and cost-effective powder disperser for aerosol particle size measurement, *Powder Technol.*, 2008, **187**(1), 27–36.

42 A. J. Tiwari, J. R. Morris, E. P. Vejerano, M. F. Hochella Jr. and L. C. Marr, Oxidation of C_{60} aerosols by atmospherically relevant levels of O_3, *Environ. Sci. Technol.*, 2014, **48**(5), 2706–2714.

43 I. Eliasson, B. Offerle, C. S. B. Grimmond and S. Lindqvist, Wind fields and turbulence statistics in an urban street canyon, *Atmos. Environ.*, 2006, **40**(1), 1–16.

44 L. F. O. Silva and K. M. da Boit, Nanominerals and nanoparticles in feed coal and bottom ash: implications for human health effects, *Environ. Monit. Assess.*, 2011, **174**(1–4), 187–197.

45 W. Abdul-Razzaq and M. Gautam, Discovery of magnetite in the exhausted material from a diesel engine, *Appl. Phys. Lett.*, 2001, **78**(14), 2018–2019.

46 E. V. Sokol, N. V. Maksimova, N. Volkova, E. Nigmatulina and A. Frenkel, Hollow silicate microspheres from fly ashes of the Chelyabinsk brown coals (South Urals, Russia), *Fuel Process. Technol.*, 2000, **67**(1), 35–52.

47 A. Bhattacharjee, H. Mandal, M. Roy, J. Kusz and W. Hofmeister, Physical characteristics of fly ashes from three thermal power plants in west bengal, India: A comparative study, *Int. J. Chem. Technol.*, 2013, **5**, 836–843.

48 N. Zajzon, E. Marton, P. Sipos, F. Kristaly, T. Nemeth, V. Kis-Kovacs and T. G. Weiszburg, Integrated mineralogical and magnetic study of magnetic airborne particles from potential pollution sources in industrial-urban environment, *Carpath. J. Earth Env.*, 2013, **8**(1), 179–186.

49 B. A. Maher, C. Moore and J. Matzka, Spatial variation in vehichle-derived metal pollution identified by magnetic and elemental analysis of roadside tree leaves, *Atmos. Environ.*, 2008, **42**, 364–373.

50 J. Matzka and B. A. Maher, Magnetic biomonitoring of roadside tree leaves: identification of spatial and temporal variations in vehicle-derived particulates, *Atmos. Environ.*, 1999, **33**(28), 4565–4569.

51 C. Carvallo, P. Sainctavit, M. A. Arrio, N. Menguy, Y. H. Wang, G. Ona-Nguema and S. Brice-Profeta, Biogenic vs. abiogenic magnetite nanoparticles: A XMCD study, *Am. Mineral.*, 2008, **93**(5–6), 880–885.

52 M. F. Hochella, S. K. Lower, P. A. Maurice, R. L. Penn, N. Sahai, D. L. Sparks and B. S. Twining, Nanominerals,

mineral nanoparticles, and earth systems, *Science*, 2008, **319**(5870), 1631–1635.

53 M. Chen, F. S. Zhang and J. Zhu, Environmental leaching characteristics and bioavailabilities of waste cathode ray tube glass, in *Recycling of electronic waste II: proceedings of the second Symposium*, ed. L. Zhang and G. K. Krumdick, Wiley, 2011.

54 C. Frazzoli, O. E. Orisakwe, R. Dragone and A. Mantovani, Diagnostic health risk assessment of electronic waste on the general population in developing countries' scenarios, *Environ. Impact. Assess Rev.*, 2010, **30**(6), 388–399.

55 A. Julander, L. Lundgren, L. Skare, M. Grander, B. Palm, M. Vahter and C. Liden, Formal recycling of e-waste leads to in-creased exposure to toxic metals: An occupational exposure study from Sweden, *Environ. Int.*, 2014, **73**, 243–251.

56 M. G. Tan, G. L. Zhang, X. L. Li, Y. X. Zhang, W. S. Yue and J. M. Chen, Comprehensive study of lead pollution in Shanghai by multiple techniques, *Anal. Chem.*, 2006, **78**(23), 8044–8050.

57 X. Zhao, S. X. Ng, B. C. Heng, J. Guo, L. L. Ma, T. T. Y. Tan, K. W. Ng and S. C. J. Loo, Cytotoxicity of hydroxyapatite nanoparticles is shape and cell dependent, *Arch. Toxicol.*, 2013, **87**(6), 1037–1052.

58 Q. Fan, Y. E. Wang, X. Zhao, J. S. C. Loo and Y. Y. Zou, Adverse biophysical effects of hydroxyapatite nanoparticles on natural pulmonary surfactant, *ACS Nano*, 2011, **5**(8), 6410–6416.

59 R. Merget, T. Bauer, H. U. Kuepper and S. Philippou, Health hazards due to the inhalation of amorphous silica, *Arch. Toxicol.*, 2002, **75**(11–12), 625–634.

60 W. Cho, M. Choi, B. S. Han, M. Cho, J. Oh, K. Park, S. J. Kim, S. H. Kim and J. Jeong, Inflammatory mediators induced by intratracheal instillation of ultrafine amorphous silica particles, *Toxicol. Lett.*, 2007, **175**(1–3), 24–33.

61 Z. Du, D. Zhao, L. Jiang, G. Cui, M. Jin, Y. Li, X. Liu, Y. Liu, H. Du, C. Guo, X. Zhou and Z. Sun, Cardiovascular toxicity of different size amorphous silica nanoparticles in rats after intratracheal instillation, *Cardiovasc. Toxicol.*, 2013, **13**(3), 194–207.

62 R. A. French, N. Monsegue, M. Murayama and M. F. Hochella, Jr., The structure a nd transformation of the nanomineral schwertmannite: A synthetic analog representative of field samples, *Phys. Chem. Miner.*, 2013, **41**(4), 237–246.

63 M. F. Hochella, Jr., J. N. Moore, C. Putnis, A. Putnis, T. Kasama and D. D. Eberl, Direct observation of heavy metal-mineral association from the Clark Fork River Superfund Complex: Implications for metal transport and bioavailability, *Geochim. Cosmochim. Acta*, 2005, **69**, 1651–1663.

544 | *Environ. Sci.: Nano*, 2016, **3**, 534–544

This journal is © The Royal Society of Chemistry 2016